

## CONSTRUCTIONAL CANYONS BUILT BY SHEET-LIKE TURBIDITY CURRENTS: OBSERVATIONS FROM OFFSHORE BRUNEI DARUSSALAM

KYLE M. STRAUB\*<sup>1</sup> AND DAVID MOHRIG<sup>2</sup>

<sup>1</sup>*Department of Earth, Atmospheric, and Planetary Sciences, Massachusetts Institute of Technology, 77 Massachusetts Avenue, Building 54-824, Cambridge, Massachusetts 02139, U.S.A.*

<sup>2</sup>*Department of Geological Sciences, The University of Texas at Austin, Austin, Texas 78712, U.S.A.  
e-mail: kmstraub@umn.edu*

**ABSTRACT:** Formation and deepening of submarine canyons are typically attributed to erosion. We present data from an industry-grade seismic volume located offshore Brunei Darussalam illustrating how topography typically associated with erosion can be produced under conditions of net sediment deposition. These data were generated via subsurface mapping in the vicinity of a shale-cored anticline on the Quaternary continental slope. The shale ridge is located 20 km down slope from the present-day continental shelf edge in ~ 900 m of water. Its crest line runs for 18 km and is oriented perpendicular to the regional slope. Three canyons traverse the structure at right angles to the crest line, with maximum canyon relief of 165 m. Subsurface mapping reveals that the structure is a site of net sediment deposition and defines a background sedimentation pattern that decreases gradually with distance from the shelf edge. Profiles down canyon axes reveal several local minima in deposit thickness over the anticline hinge that are associated with high downstream gradients. Deposition on ridges adjacent to canyons also displays local minima at the anticline hinge, but these minima are not correlated with gradient. A comparison of canyon axis and ridge deposition shows that somewhat higher rates of sedimentation on the ridges resulted in the preservation and growth of the submarine canyons with time. Laterally persistent seismic reflectors and depositional packages suggest that the canyon forming currents were sheet-like flows, extending for many kilometers in the strike direction. This interpretation is consistent with minima in ridge deposition being correlated with maximum canyon relief. The currents drained into canyons as they approached the anticline hinge, leaving only a small supra-canyon fraction available to deposit sediment on the nonchanneled zones. We use the cross-sectional area of the confined flow over the anticline crest to estimate a minimum thickness of 20 m for the sheet-like currents as they approached the anticline.

### INTRODUCTION

The collection of high-resolution bathymetric maps in the last two decades has revealed many previously unrecognized morphological features in the deep-marine environment (Piper and Normark 1983; Stelling et al. 1985; Pratson et al. 1994; Pirmez and Flood 1995; Pratson and Haxby 1996). Advances in imaging of the seafloor are the result of advances in geophysical exploration technologies that include multibeam sonar systems and three-dimensional (3-D) seismic surveys. Many seafloor features have morphometric properties that are similar to better studied terrestrial topography (Pirmez 1994; Imran et al. 1999; Posamentier and Kolla 2003). This similarity has motivated numerous investigations of continental-margin morphodynamics (Kneller and Pratson et al. 1994; Buckee 2000; Pirmez et al. 2000; Goff 2001), and many of these studies have employed quantitative process models developed for terrestrial systems to evaluate the evolution of submarine systems (Komar 1969; Greene et al. 2002; Pirmez and Imran 2003; Mitchell 2005; Mitchell 2006). Channel and canyon systems on continental slopes have received the greatest attention (Peakall et al. 2000; Pirmez and Imran 2003; Skene et al. 2002; Fildani and Normark

2004). These conduits display a range of configurations shared by their terrestrial counterparts, including tributary and distributary channel networks (Pratson et al. 1994; Cunningham et al. 2005; Garcia et al. 2005; Mitchell 2005; Straub et al. 2007). Unfortunately, the great water depths at which many of these systems exist and the infrequent occurrence of flow in submarine channels and canyons has limited the number of direct observations defining the processes that evolve the submarine landscape (Hay 1987; Khripounoff et al. 2003; Xu et al. 2004; Best et al. 2005). In several regions, maps of the present-day seafloor are the only data available with which to evaluate continental-slope dynamics. In this work, we use an industry-grade 3-D seismic survey to observe the growth of a canyon system as recorded in the deep-marine strata. We document the limitations to importing process models for canyon development in terrestrial systems to the deep-marine environment.

Submarine canyons are common features on continental margins, and they share many common attributes with terrestrial canyons (Canals et al. 2000; Greene et al. 2002). These canyons are defined by high-relief, V-shaped valleys with steep sidewalls. Many also have irregular floors defined by large dunes (Smith et al. 2005) and knickpoints (Mitchell 2006; Lamb et al. 2008). The heads of most submarine canyons are linked to the continental shelf-slope break and can sometimes extend landwards across the shelf, even into feeding river mouths (Greene et al. 2002). Many canyons, though, begin tens of kilometers downslope from the shelf edge

\* Present Address: Department of Geology and Geophysics, University of Minnesota, Minneapolis, Minnesota 55414, U.S.A.

(Demyttenaere et al. 2000; Pirmez et al. 2000; Huyghe et al. 2004; Bertoni and Cartwright 2005; Cunningham et al. 2005). These canyons typically start at regions where the continental-slope gradient undergoes a rapid change (Demyttenaere et al. 2000; Goff 2001; Huyghe et al. 2004), often associated with structural deformation that includes faulting and folding by mobile substrate (Demyttenaere et al. 2000; Pirmez et al. 2000; Huyghe et al. 2004). All of these canyons are assumed to be areas of net erosion (Canals et al. 2000; Bertoni and Cartwright 2005; Cunningham et al. 2005).

Direct observations (Burbank et al. 1996; Burbank et al. 1999; Snyder et al. 2000; Formento-Trigilio et al. 2002) and theoretical modeling (Burbank et al. 1996; Tucker and Slingerland 1996; Humphrey and Konrad 2000) of interactions between terrestrial channels and regions of local uplift have guided the study of submarine-canyon evolution. In the terrestrial system, channels respond to regions of local uplift in one of three ways: (1) diversion around the region of uplift; (2) by depositing sufficient amounts of sediment both upstream and downstream of the uplift to suppress development of a structural high; or (3) incision through the region of uplift, creating a canyon (Burbank et al. 1996; Humphrey and Konrad 2000). The pathway of river response to regions of local uplift depends on the stream power, the sediment load of the river, and the rate of local uplift, and the erodibility of uplifted strata (Burbank et al. 1999; Snyder et al. 2000). To follow the incision path, a channel must erode its bed at a rate equal to or greater than the rate of regional uplift; therefore all terrestrial canyons are the result of net erosional processes.

Turbidity currents differ from terrestrial channelized flows in several ways that substantially alter how they interact with topography. A critical difference between the two flow types is the density of the ambient fluid through which they flow. Ocean water is roughly 800 times denser than air. As a result of this difference in ambient fluid density, turbidity currents are less influenced by changes in topography than rivers (Kneller et al. 1991; Lamb et al. 2006; Straub et al. 2008). This difference in ambient fluid density also allows the thickness of turbidity currents to be several times greater than the channels that guide them (Mohrig and Buttle 2007), a situation that seldom if ever occurs in the terrestrial environment. Because of this difference, rivers are always strongly channelized compared to submarine flows. Evidence from several studies suggests some turbidity currents that move down continental margins are poorly channelized (Field et al. 1999; Pickering et al. 1992; Spinnelli and Field 2001; Wright et al. 1988; Wynn et al. 2000a; Wynn et al. 2000b). These currents are referred to as sheet flow or sheet-like currents and are interpreted to have ratios of current width to thickness in excess of 1000 (Field et al. 1999; Booth et al. 2000; Twitchell et al. 2005; Violet et al. 2005). These sheet flows have not been directly observed traveling down the continental slope, but outcrop and seismic studies suggest that they contribute a substantial amount of the sediment to continental margins, aiding progradation of clinoforms (Wright et al. 1988; Pickering et al. 1992). Significant quantitative advances have been made in our understanding of the processes and morphodynamics of channelized submarine flow (Imran et al. 1999; Pirmez and Imran 2003; Imran et al. 2004; Keevil et al. 2006; Straub et al. 2008). Little, however, is currently known about how sheet-flow currents interact with topography to evolve the seascape. We examine the construction of topography by apparent sheet-like turbidity currents on the northern continental margin of Borneo, offshore Brunei Darussalam.

#### CONTINENTAL MARGIN, OFFSHORE BRUNEI DARUSSALAM

The morphology of the present-day continental slope offshore Brunei Darussalam is primarily influenced by the progradation of deltaic depocenters situated at its margin (Saller and Blake 2003; Hutchison 2004; Morley 2007). Sediment is delivered to the margin primarily through three river systems, the Baram, Belait, and Tutong rivers (Sandal

1996; Hiscott 2001; Hutchison 2004). High sediment discharge from these river systems has resulted in the construction of a continental shelf that is 50–70 km wide and underlain by 8–10 km of siliciclastic sediments. Using mapped seismic horizons tied to wireline log data and biostratigraphic dating Saller and Blake (2003) estimated that the Brunei shelf edge has prograded 80 km since the middle Miocene. Beginning in the late Miocene progradation was highest along the northeast part of the Brunei shelf associated with the growth of the Champion Delta. The locus of deposition shifted to the southwest during the early Pliocene, associated with the growth of the Baram Delta. The change in deposition locus probably resulted from a capturing of substantial parts of the Champion Delta hinterland drainage by the Baram River (Saller and Blake 2003). Shelf-margin progradation during the Quaternary has been relatively rapid at 11 km/My (or a total progradation of 20 km). Quaternary deposits have been thickest in the southwest associated with lowstand deltas (Saller and Blake 2003). Of the three rivers, the Baram currently has the largest drainage-basin area and water and sediment discharges,  $0.0192 \times 10^6 \text{ km}^2$ ,  $1445 \text{ m}^3/\text{s}$ , and  $2.4 \times 10^{10} \text{ kg/yr}$ , respectively. The sediments are derived from erosion of uplifted rocks from the Rajang–Crocker ranges in central Borneo. Erosion rates measured in these ranges are amongst the highest in the world and have resulted in high sedimentation rates in the South China Sea since the Eocene (Hutchison 2004; Sandal 1996).

Offshore Brunei Darussalam, the continental shelf–slope break occurs at a water depth of ~200 m (Fig. 1). From that position the seabed descends steeply until reaching the floor of the Borneo Trough at a water depth of 2800 m. The upper slope is characterized by a relatively steep average gradient of 0.038 m/m (Demyttenaere et al. 2000; McGilvery and Cook 2003). Its southwestern margin is characterized by a pair of prominent shelf-edge-parallel ridges with canyons traversing the ridges. These strike-parallel ridges are the product of diapirism by mobile overpressured shale that is rising into overlying sediments along faults (van Rensbergen et al. 1999; Demyttenaere et al. 2000; Ingram et al. 2004; Morley 2007). Our study focuses on the second of these ridges and three canyons that traverse it.

Exploration and production of hydrocarbons has occurred on the Brunei continental slope for over 20 years. Sediments deposited on the continental margin since the Pliocene, as confirmed by well penetrations, range between clays and sands and include a high fraction of sediments interpreted as turbidites (Sandal 1996). Turbidites on the continental slope of Brunei have been identified in both relatively unconfined (Sandal 1996) and relatively confined (channel) settings (Demyttenaere et al. 2000; Straub and Mohrig in press). A large oil and gas field exists between our study area and the shelf edge, termed the Merpati Field. The present-day water depth above this reservoir is 458 m. Well penetrations have identified thick sandstones in this region, interpreted as turbidites deposited in a relatively unconfined setting (Sandal 1996). Biostratigraphic data of nannofossils and foraminifera from exploration wells on the upper continental slope suggest deposition rates of 40–50 cm/kyr during the Quaternary (Hiscott 2001).

Few measurements of ocean currents are available for offshore Brunei. Data available, however, suggest complex flow patterns, both surface and deep water. In the offshore region, the Southwest Monsoon dominates the current patterns, with primary flow directions toward the northeast (shoreline parallel). Occasional strong currents with flow direction perpendicular to the shoreline have also been identified. These latter currents have been interpreted as internal waves traveling at depth across the deep central section of the South China Sea. The internal waves occasionally hit the shelf and transport colder deep water onto the shelf (Sandal 1996).

#### Seismic Data Set Parameters

To carry out this study we have taken advantage of access to a large, industry-grade 3-D seismic volume collected on the continental slope

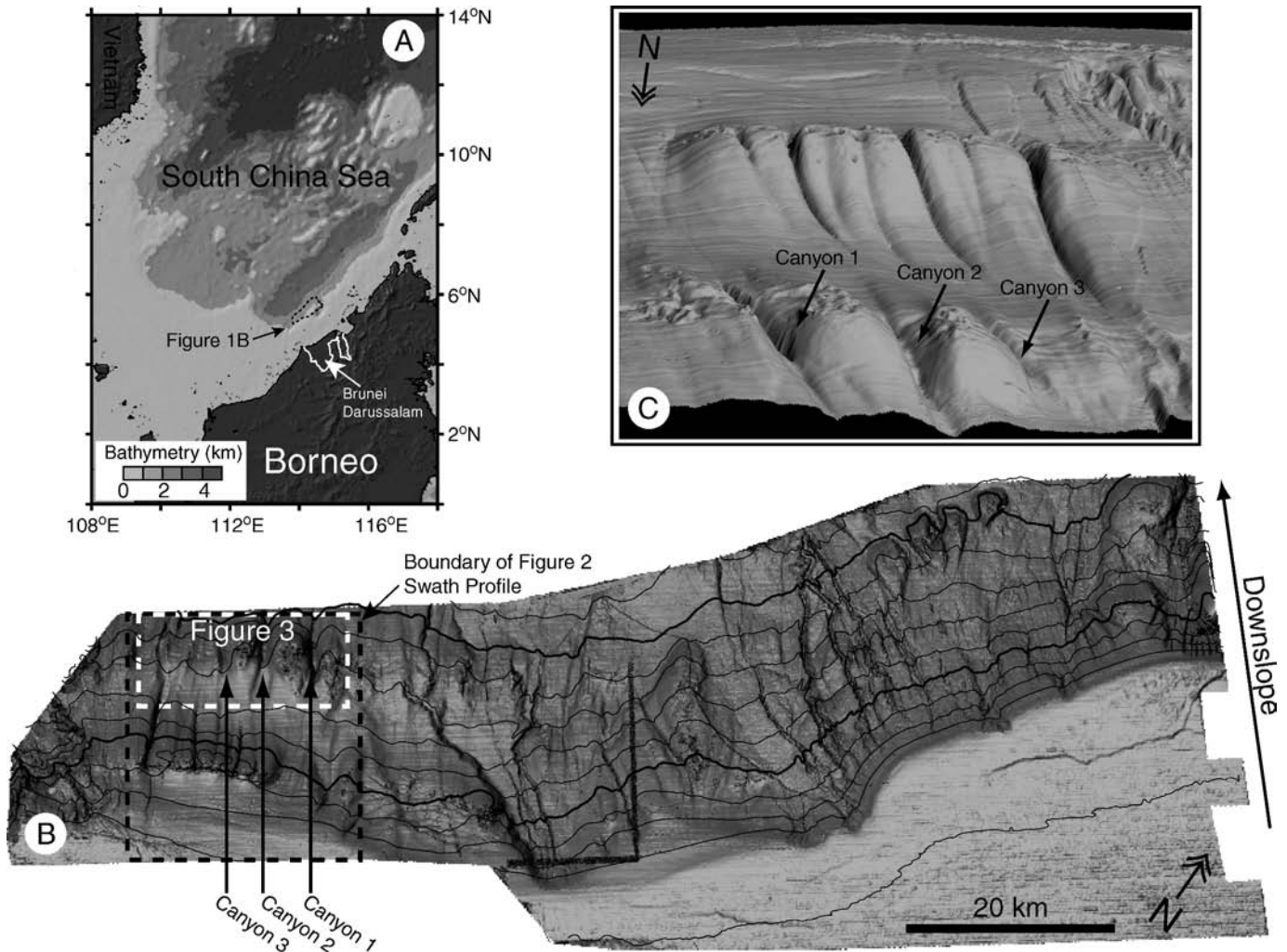


FIG. 1.—Location maps and 3-D perspective of study region. **A)** Bathymetric map of the South China Sea, with location of study region marked by dashed box. **B)** Slope map of continental shelf and slope, offshore Brunei Darussalam. Contour interval = 100 m water depth. The black dashed line defines the area used to calculate the swath profiles presented in Figure 2. The white dashed line defines the area studied using 3-D seismic volume. **C)** 3-D perspective view of study region with Canyons 1, 2, and 3 labeled. Topography is vertically exaggerated by a factor of 3.

offshore Brunei Darussalam covering an area of  $4000 \text{ km}^2$  ( $40 \text{ km} \times 100 \text{ km}$ ). This study focuses on a subset of the 3-D seismic survey, an area of  $200 \text{ km}^2$ , which encompasses the shelf-edge-parallel anticlines shown in Figure 1. Present-day water depths increase from approximately 550 m to 1050 m moving from the proximal to distal end of the study region. We focus on the sedimentary section imaged by the first 0.3 seconds of two-way travel time (TWT) beneath the seafloor. For this portion of the 3-D data volume, the frequency roll-off is near 80 Hz, providing a vertical resolution in deposit thickness of approximately 3 m. The horizontal resolution is limited by  $25 \text{ m} \times 25 \text{ m}$  spacing between lines of the seismic grid.

#### Shale Diapirism

Two prominent ridges occur within the study area. Both are oriented roughly parallel to the present-day shelf-slope break. The average bathymetric profile of the downslope surface topography for this region of the shelf and slope encompassing these ridges is presented in Figure 2A, and its associated surface gradient is plotted as Figure 2B. This average profile is a swath profile calculated from a set of evenly spaced, parallel profiles that are oriented in the dominant downslope

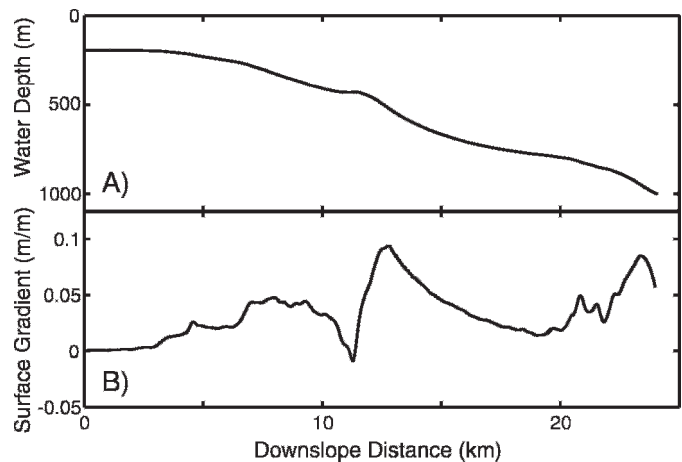


FIG. 2.—**A)** Bathymetry and **B)** downslope surface gradient for the swath profile covering the area marked in Figure 1B.

direction. Downslope gradient is calculated at each node using the elevation difference between its upslope and downslope neighboring bins. The two shelf-edge-parallel ridges create a stepped profile with low surface gradients upstream of the ridges and high surface gradients directly downslope of the ridge crests. These ridges are the product of shale diapirs (van Rensbergen et al. 1999; Demyttenaere et al. 2000). Mobile shale generally is derived from buried, laterally extensive depositional sequences that are in excess of a hundred meters thick, where a combination of high sedimentation rates and low permeability inhibit the flow of interstitial water and cause pore-fluid pressures to rise above hydrostatic levels (Westbrook and Smith 1983; van Rensbergen et al. 1999). Miocene to present loading of sediment associated with the progradation of the Baram Delta over a thick, shale-prone marine sequence of Oligo-Miocene age called the Setap Shale produced the conditions for mobile shales and diapirism in the study area (Sandal 1996; van Rensbergen et al. 1999). Active diapir growth in this region occurred until the late Pliocene or early Pleistocene (Demyttenaere et al. 2000). On seismic data, the mobile shale is identified as low-velocity, chaotic to reflection-free intervals that are not necessarily confined by stratigraphic units (Westbrook and Smith 1983).

### 3-D SEISMIC GEOMORPHOLOGY OF THE SHALE RIDGE

#### *Map Trends*

The present-day seafloor in our study area was picked on each in-line of the seismic volume (Fig. 3A). We also mapped four shallow regional surfaces, named SR1, SR2, SR3, and SR4 in order of increasing depth below the present-day seafloor (Figs. 4, 5). These subsurface seismic horizons were selected for mapping because they had strong reflection amplitudes that could be tracked regionally over the full extent of the study region. This interval overlies mobile shale that is characterized by zones of low reflectivity and chaotic reflectors in seismic cross sections and time slices (Figs. 3B, 4). Biostratigraphic dating provided from samples collected at petroleum exploration wells located near the study area coupled to the high progradation rates of the Quaternary margin over the thick Setap Shale suggests that our entire mapped interval is at minimum of Quaternary age (Hiscott 2001). Maps of the four subsurface seismic horizons represent approximate realizations of four paleo-seafloor configurations. When used in conjunction with the present-day seafloor map, they allow us to evaluate how sediment deposition has caused the seafloor to evolve through time.

Present-day water depths over the studied shale ridge range between 550 m and 1050 m (Fig. 3A). Three canyons traverse this ridge. Canyon relief is defined here as the difference in elevation between the canyon axis or thalweg and the average of the elevations for the overbank surfaces that bound each side of the feature (Figs. 3A, 6). The maximum relief for canyons 1, 2, and 3 are 161 m, 140 m, and 75 m, respectively. This maximum relief for the canyon systems occurs close to the hinge line of the shale ridge (Fig. 3B). Upslope and downslope from the shale ridge the three canyon systems lose almost all of their relief. With the exception of several low-relief linear scours, the regions upslope and downslope of the canyon axis can be characterized as nonchannelized. A map of average local surface gradient was created using the present-day seafloor bathymetry (Fig. 3C). This surface gradient was calculated at every seismic bin by averaging the absolute gradient measured between the eight neighboring bins. The highest surface gradients are associated with the sidewalls of canyons and the downslope limb of the shale ridge. The lowest surface gradients are located directly updip from the shale ridge in the nonchannelized region.

The five mapped horizons have been converted from TWT to elevation below mean sea level using a seismic velocity of 1460 m/s for seawater and 1700 m/s for the shallow deposit. This seismic velocity for the first 300 m of sedimentary deposits beneath the seafloor was taken from a petroleum-

well control point located in our study region (van Rensbergen et al. 1999). The approximate paleo-seafloor topography recorded in seismic horizons SR1–SR4 contain most of the features found on the present-day seafloor (Fig. 7). Topography associated with the shale ridge is observed in each map, with low surface gradients and high surface gradients located upslope and downslope of the shale-ridge hinge line, respectively. Several differences between the present-day seafloor and the paleo-seafloors are noted. First, the relief of the channel–levee system located in the extreme southwestern portion of the survey has decreased through time. Second, the maximum relief for all three canyons has increased through time. Unfortunately the quality of the seismic data below horizon SR4 precludes mapping of deeper horizons. As such we cannot evaluate the mechanisms that started canyon growth in the study region.

Maps of deposit thickness were created by differencing seafloor and subsurface horizons (Fig. 8). These maps indicate that the study region is everywhere a site of net sediment accumulation. The first-order trend is a systematic decrease in deposit thickness with increasing downslope distance. Superimposed on this trend are relative lows in sediment deposition associated with the canyon thalwegs that traverse the shale ridge, and a local maximum in deposit thickness is associated with the filling of the channel–levee system located in the southwestern portion of the study region.

Swath profiles characterize how overall deposit thickness varies as a function of the downslope distance (Fig. 9). Average deposit thickness decreases as a function of distance from the shelf edge. Figure 9B shows that excluding a local effect of the shale-cored anticline, overall deposit thickness decreases linearly at 9 m/km in the downslope direction. A local minimum in deposit thickness is associated with the hinge line of the shale ridge. Interestingly, the increase in deposit thickness observed immediately downslope of the shale-ridge hinge line is spatially correlated with the largest measured surface gradients for the long profile of the system (Fig. 9C).

#### *Comparison of Canyon Axis and Confining Overbank Surfaces*

To separate the contributions of canyons and overbank surfaces to the average deposit thickness trend, swath profiles were analyzed from each of these regions independently. First, properties of Canyon 1 (Fig. 1C) were analyzed along a 0.5-km-wide transect labeled C1 in Figure 3A. The swath profiles of canyon bathymetry, downslope gradient, and deposit thickness were calculated for this transect and are plotted in Figure 10A. Properties of the overbank to either side of the canyon are for the 0.5-km-wide transects labeled O1 and O2 in Figure 3A. The overbank profile locations are centered on the topographic highs adjacent to the canyon. Swath profiles for O1 and O2 are calculated and then averaged to produce the characteristic bathymetry, downslope gradient, and deposit thickness associated with the adjacent overbank surface (Fig. 10B). Present-day seafloor gradients also presented in Figure 10 are measured using a 150 m moving window centered on each analyzed bin.

Swath bathymetry shows a stepped-slope topography associated with the axis of Canyon 1 as it traverses the shale ridge (Fig. 10A-1). The two steps are characterized by extreme downslope gradients of 0.25 m/m and 0.09 m/m respectively. Swath profiles of deposit thickness along the canyon axis show local minimums centered over the shale-ridge hinge line. The amplitude of this local minimum systematically increases as total sediment thickness increases between horizons SR4 and the present-day seafloor (SR0).

Mean bathymetry of the overbank surface that confines Canyon 1 smoothly increases at a gradient of 0.013 0.009 m/m updip from the shale-ridge hinge-line and an average gradient of 0.073 0.002 m/m downslope of the hinge-line (Figs. 10B-1, 10B-2). Local minimums in the swath profiles for overbank-deposit thickness are centered on the shale-ridge hinge line (Fig. 10B-3). This thickness distribution is consistent with what is observed for the canyon-axis profiles (Fig. 10A-3).

An identical set of measurements and calculations was made for Canyon 2 (Fig. 1C) using transects C2, O2, and O3 (Fig. 3A). Results for

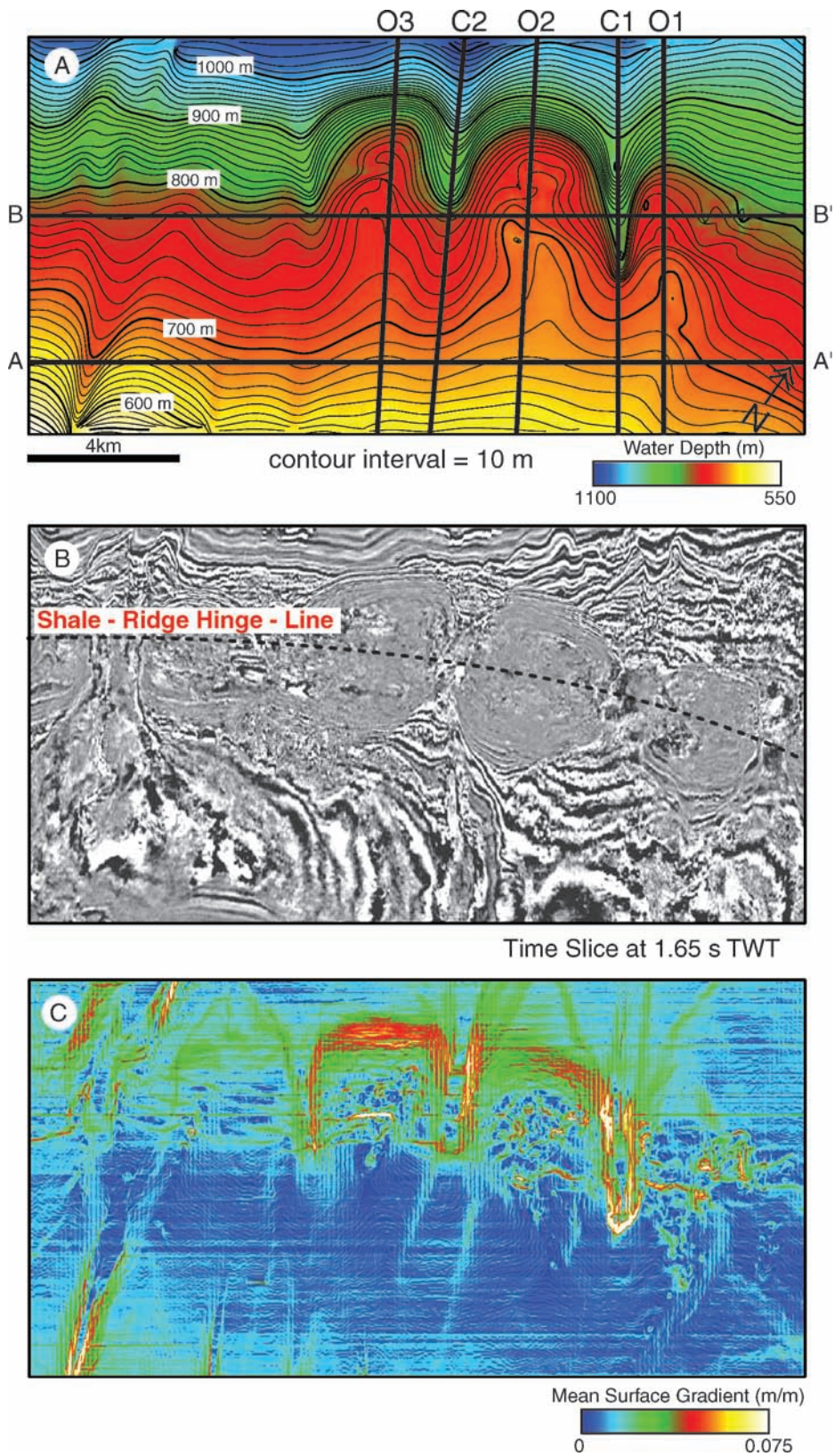


FIG. 3.—Area studied using 3-D seismic volume. The position of the 3-D seismic volume is marked in Figure 1B. **A**) Map of present-day seafloor with 10 m bathymetric contours. Strike cross sections A-A' and B-B' define locations of seismic cross-sections displayed in Figure 4. Dip cross-sections C1, C2, O1, O2, and O3 define centerlines of 0.5-km-wide swath profiles presented in Figures 10 and 11. **B**) time slice of seismic volume at 1.65 s of TWT. The dashed line marks the hinge line of the shale ridge. **C**) Map of local mean surface gradient for the present-day seafloor.

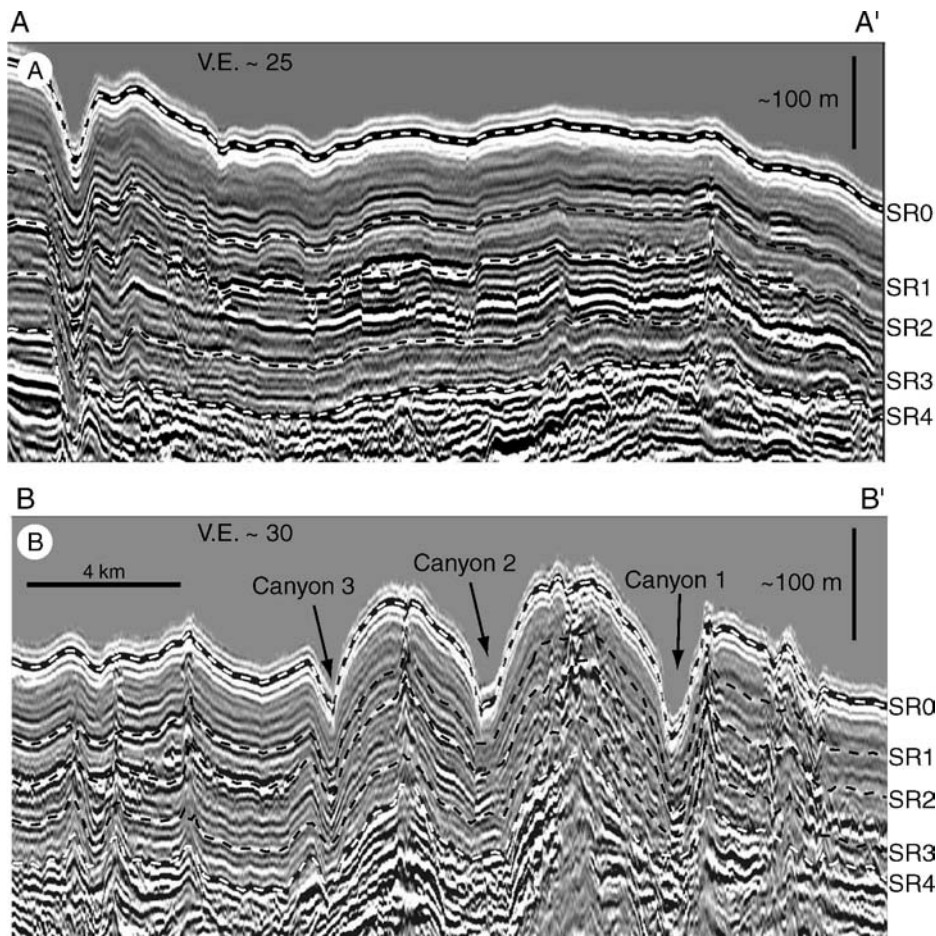


FIG. 4.—Characteristic strike-oriented seismic lines for study region. Dashed lines labeled SR0–SR4 follow the mapped surface and subsurface seismic horizons used in this study. The locations of these two seismic cross sections are marked in Figure 3A. **A)** Seismic cross section located upslope of the shale ridge. **B)** Seismic cross section at the shale ridge.

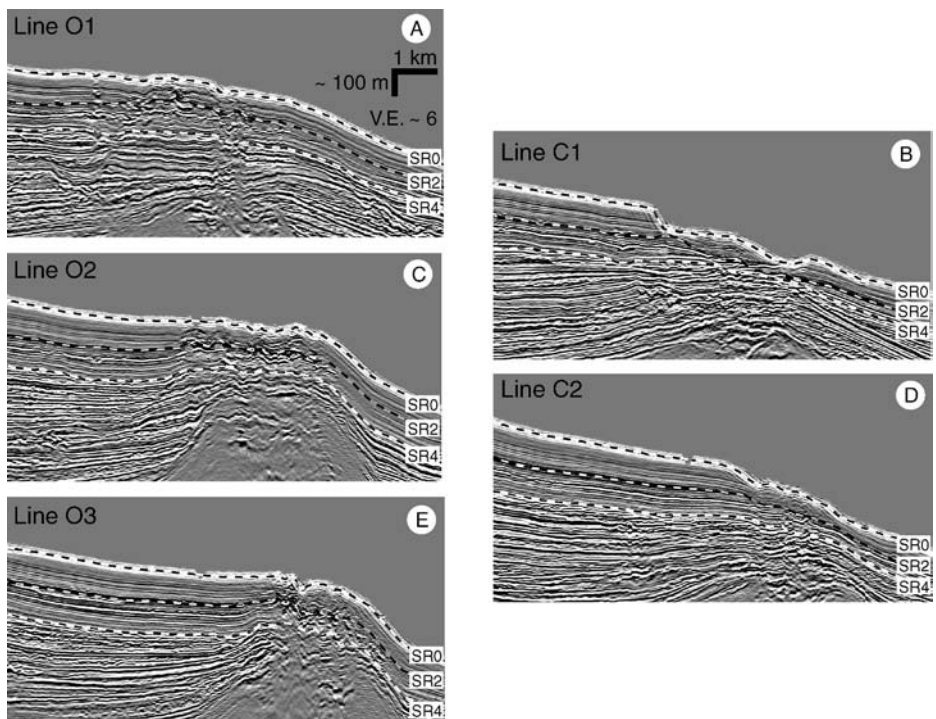


FIG. 5.—Characteristic dip-oriented seismic lines for the study region. Seismic lines move progressively from the east (A) to the west (E) and represent the eastern overbank axis of canyon 1 (A), the axis of canyon 1 (B), the inter-canyon region between canyon 1 and 2 (C), the axis of canyon 2 (D), and the western overbank axis of canyon 2 (E). Dashed lines labeled SR0–SR4 follow the mapped surface and subsurface seismic horizons used in this study. Locations for these five seismic cross sections are marked in Figure 3A.

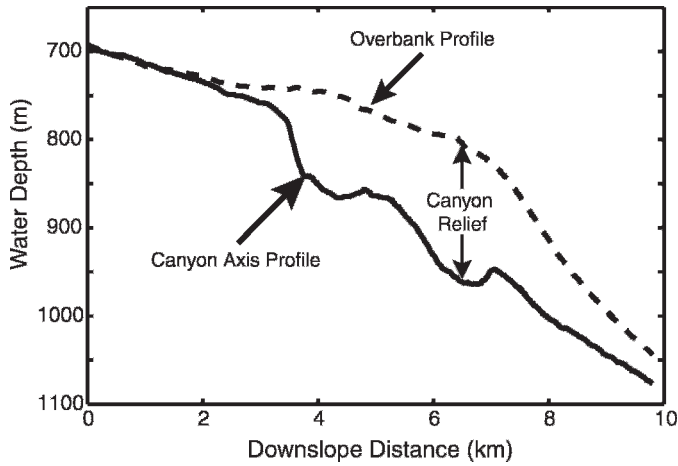


FIG. 6.—Long profile for axis of Canyon 1 (C1 of Fig. 3A) and long profile of adjacent overbank surface (average value for O1 and O2 of Fig. 3A). The vertical distance separating the two profiles is the local canyon relief.

Canyon 2 are presented in Figure 11. Similar to the Canyon 1 system, the highest sea-floor gradients along the canyon axis are measured where it traverses the shale ridge (Fig. 11A-2) and the largest sea-floor gradients associated with the mean overbank surface are measured on the downslope side of the shale ridge. The shale-ridge hinge line is associated with local lows in deposit thicknesses for both the canyon axis and the confining overbank (Figs. 11A-3, B-3).

#### INTERPRETATION

##### *Depositional Process*

Deposition of sediment on continental slopes can result from a number of different processes or a combination of processes. What was the dominant process responsible for depositing the mapped intervals of stratigraphy in our study region? The subsurface horizons SR1–SR4 persist in the strike direction across the entire study region (Fig. 4). Upslope and downslope of the shale-ridge hinge line these horizons appear to drape pre-existing topography rather than onlap older horizons. These reflectors are infrequently truncated by small channel features which have depths of less than 10 m. Further, the amplitude of

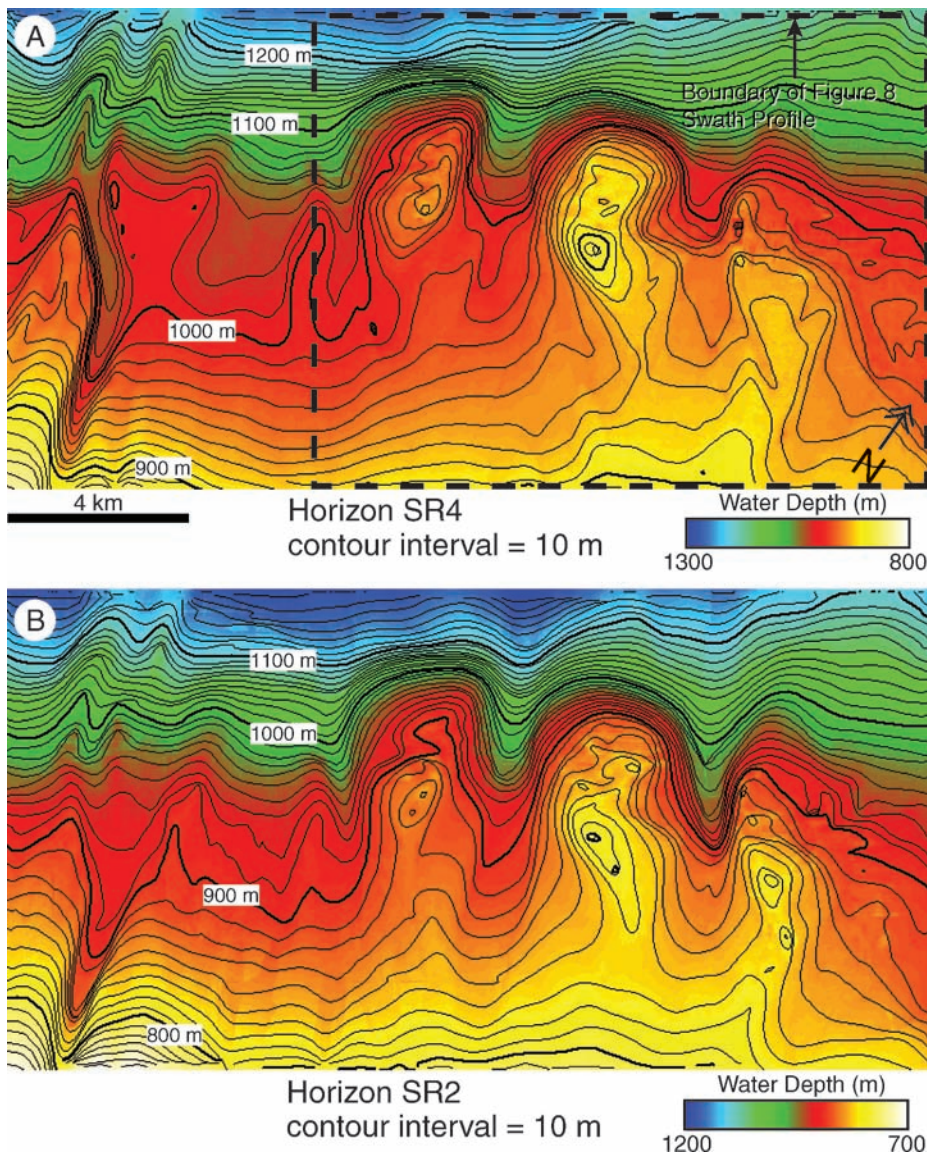


FIG. 7.—Structure maps for horizons SR4 and SR2. **A)** Structure map of horizon SR4 with 10 m contours. The black dashed line defines the region used to calculate the swath profiles presented in Figure 9. **B)** Structure map of horizon SR2 with 10 m contours.

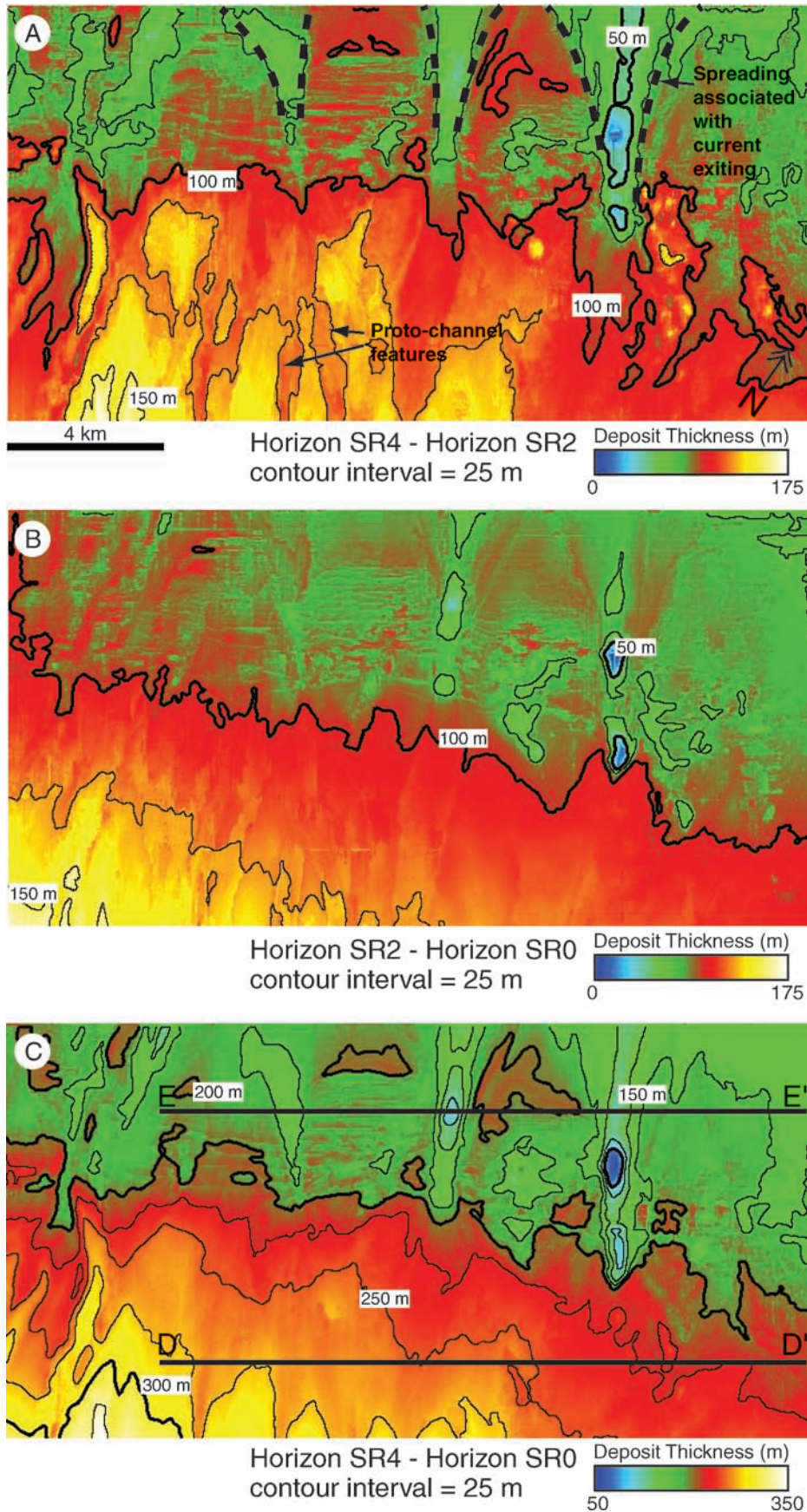


FIG. 8.—Maps of deposit thickness measured between regionally mapped seismic horizons. **A)** Deposit thickness of the section between horizons SR4 and SR2 with 10 m contours. **B)** Thickness of deposit measured between horizons SR2 and SR0 (present-day seafloor) with 10 m contours. **C)** Thickness of the sedimentary section bounded by horizons SR4 and SR0 with 10 m contours. Strike lines marked D–D' and E–E' define locations of deposit-thickness profiles in Figure 14.

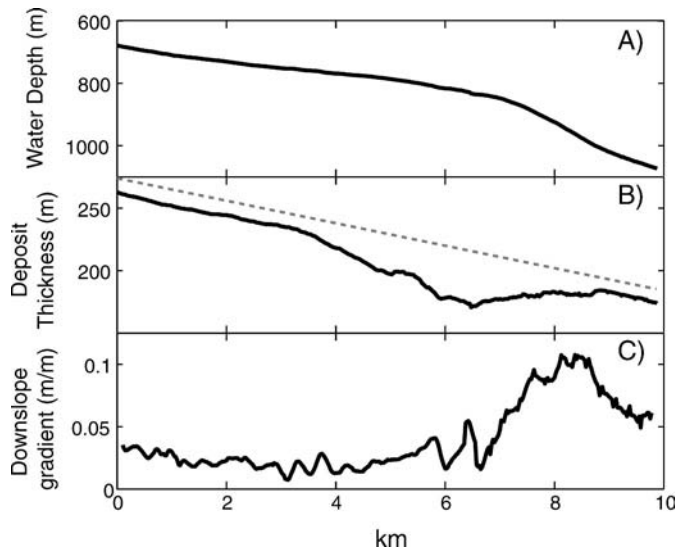


FIG. 9.—Average downslope properties of the study area marked in Figure 7A. **A)** Long profile of the area. **B)** Thickness of sedimentary section between horizons SR0 and SR4. The gray dashed line defines a deposit taper of 9 m/km. **C)** Surface gradient of the long profile in part A.

the mapped seismic horizons, when not truncated by small channels, is fairly consistent over great horizontal distances (several kilometers), suggesting a lack of sub-seismically resolvable channels.

Laterally extensive horizons which drape topography are often associated with hemipelagic deposition. Several factors, however, suggest this is not the only deposition process in our study region. Hemipelagic deposition rates summarized by Stow et al. (Stow et al. 2001) can vary greatly depending on the nature of the biogenic and terrigenous inputs. In low-latitude to mid-latitude settings rates vary between 2 cm/ky in regions with little terrigenous input to 10 cm/ky on continental margins in areas of high upwelling and biological production. A deposition rate associated with our mapped deposits can be estimated using the duration of the Quaternary, 1.8 million years, as the time span for deposition of the sedimentary package bounded by horizons SR4 and SR0. As discussed earlier, recent rapid progradation rates over the mobile Setap Shale coupled to biostratigraphic dating conducted at sites near our study area suggest a minimum age for deposits in this study of 1.8 million years; as such, our deposition rate is a lower bound. Using this method we estimate a minimum deposition rate of 17 cm/ky, greater than most hemipelagic fallout rates. In addition, the northern Borneo margin is a site of low upwelling and biological production (Laws et al. 2000), further reducing the likelihood that the mapped deposits are hemipelagites.

A turbidity-current origin for the studied deposits is also supported by the depositional patterns observed in the vicinity of the shale-ridge crest line. Maximum deposition rates on topographic highs and minimas within the canyons and the strong deposition gradient in the downslope direction are patterns that are difficult to explain if sedimentation is from a distributed fallout of fine-grained particles from the uppermost portion of the water column. On the other hand, this sedimentation pattern and the identification of turbidities deposited in unconfined settings immediately upslope of our study region suggest deposition from bottom-hugging, laterally extensive turbidity currents, as described below.

### Canyon Growth

Our five mapped horizons can be used to estimate how the relief of canyons 1 and 2 changed through time, and these relief histories are presented in Figure 12. These data show a progressive increase in the overall

relief for each canyon. For example, the maximum relief of Canyon 1 increased from about 74 m to about 159 m over the time window associated with horizons SR4 and SR0. Maximum relief for Canyon 2 increased from about 109 m to about 139 m during this same span of time. Growth in canyon relief is not axially symmetric. Increases in relief were skewed to the downslope limb of the shale-cored anticline for both canyons. This pattern of growth has caused the two canyons to lengthen downslope.

Unlike terrestrial systems, the progressive deepening of these submarine canyons occurred during net depositional conditions. For canyon relief to increase in net depositional environments the magnitude of deposition along canyon axis must be less than the sedimentation on the confining topographic highs. We propose that the relatively low deposition rates within the canyons (Figs. 13, 14) were the product of a change in flow properties as sheet-like currents funneled into the canyons from the unconfined surface positioned immediately updip. Associated with this funneling effect is a thickening of the currents. Observed sediment deposition on the topographic highs separating the canyons seems to indicate that flows in canyons exceeded 150 m in thickness. This increase in thickness and lateral confinement of the flows is hypothesized to have increased the re-entrainment rates for sediment as currents traversed the canyons. Sedimentation rates are lower within the confines of the canyons because a larger fraction of all suspended particles settling onto the bed there are immediately lifted back into the flow interior. Additional processes other than turbidity currents might also aid the reduction in sedimentation rate in these canyons. Several studies have shown that internal tides can initiate sediment transport on continental slopes (Ribbe and Holloway 2001; Cacchione et al. 2002). Occasional internal tides have been observed on the northern Borneo margin (Sandal 1996), and funneling of these tides through canyon topography might facilitate flushing of sediment out of the canyons.

The measured patterns of sedimentation of the ridges separating the canyons (Figs. 13, 14) are consistent with laterally extensive currents funneling into these conduits while traversing the shale-cored anticline (Figs. 10B-3, 11B-3). We interpret the reduction in sedimentation leading up to the position of the hinge line as an expression of collection of the current into the canyon. As canyon relief increases toward the hinge line there is ever less supra-canyon current available to deposit sediment on the intervening highs. This trend reverses downslope of the hinge line as canyon relief begins to decrease, transferring an ever increasing fraction of the total current onto the overbank surface, where it contributes to increasing sediment deposition. As with the canyon axis, low sedimentation rates on the overbank crest of the anticline might also be affected by motion of internal tides interacting with topographic highs. We suggest that currents being collected and expelled from canyons is the dominant control on patterns of inter-canyon sedimentation. This proposal is supported by the unlikely spatial correlation between the largest downslope surface gradients (Figs. 10B-2, 11B-2) and the thickest inter-canyon sediment accumulations (Figs. 10B-3, 11B-3). Highest deposition rates on the steepest slopes are counterintuitive unless otherwise offset by an increasing volume of current becoming available to contribute to this sedimentation as the flows begin leaving the canyons.

It is worth noting that the westernmost channel in the study area possesses a different sedimentation pattern than the one already described for canyons 1, 2, and 3. This westernmost channel (Fig. 1) displays greatest rates of sediment deposition of the channel bottom and a loss of channel relief through time (Fig. 8). We propose that the explanation for this difference is connected to the entrance condition for the westernmost channel. The westernmost channel is directly connected to an up-dip canyon. Because of this, sediment gravity flows are able to enter the study area without experiencing a loss of lateral confinement. This mode of arrival is the opposite of conditions at the heads of Canyons 1, 2, and 3, where gravity currents must traverse a laterally unconfined surface. We

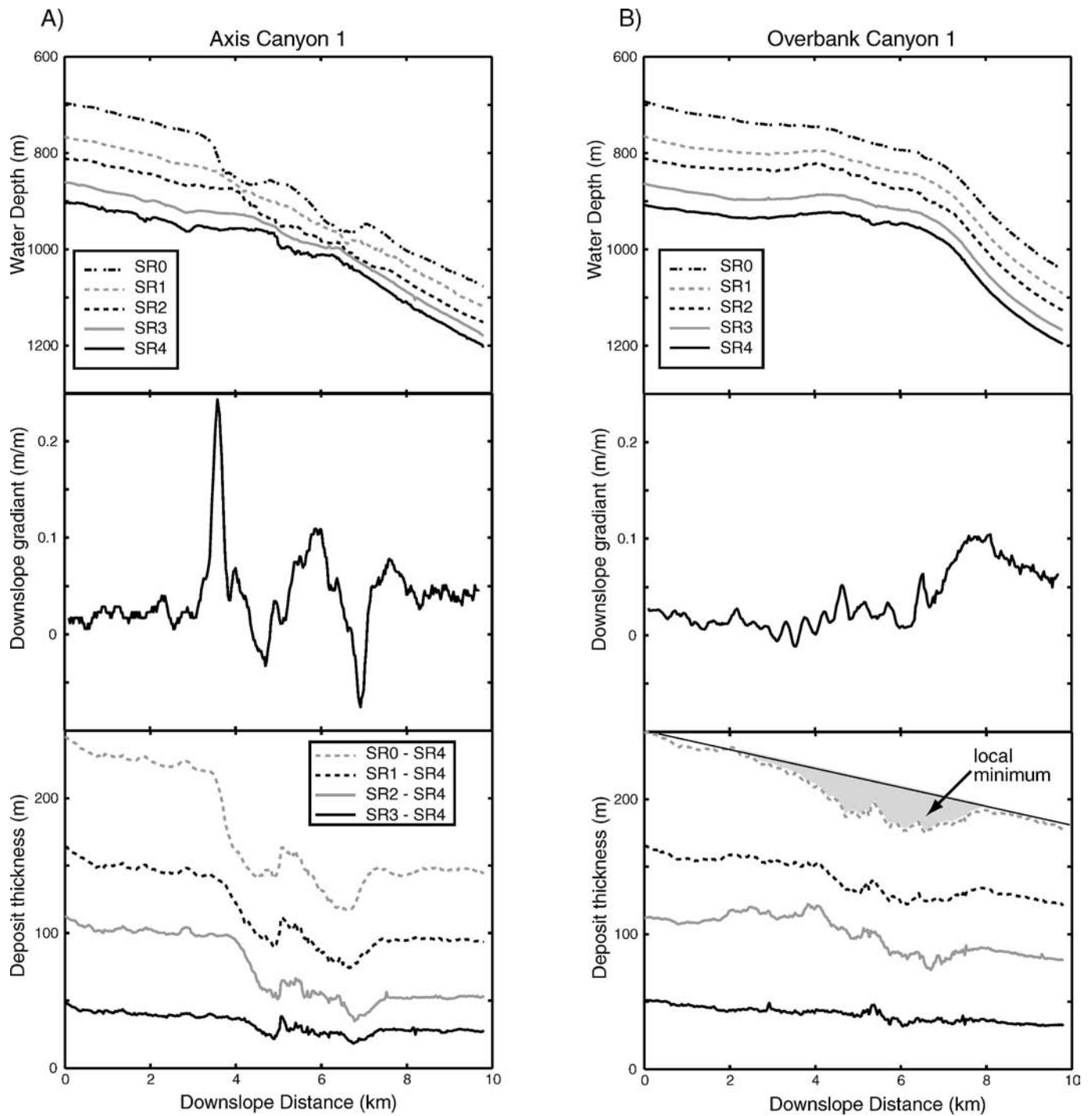


Fig. 10.—Comparison of properties for Canyon 1 and adjacent overbank at the shale ridge. **A-1)** Long profiles for seismic horizons SR4–SR0 following swath C1 (Fig. 3A) and the present-day axis of Canyon 1 (Fig. 1C). **A-2)** Surface gradient for long profile of horizon SR0, the present-day seafloor, following the axis of Canyon 1. **A-3)** Deposit thickness measured between horizons SR4–SR1 along swath C1, the axis of Canyon 1. **B-1)** Representative long profiles for the overbank surface laterally adjacent to Canyon 1. Each profile represents the average elevation for seismic horizons SR4–SR0 along transects O1 and O2 (Fig. 3A). **B-2)** Downslope gradient of present-day seafloor associated with the average overbank profile in (B-1). **B-3)** Deposit thickness associated with successive long profiles in part B-1. The shaded region defines local minima in overbank sedimentation. See text for details.

suggest that this difference in confinement preserved a suspended-sediment profile with different characteristic properties. Specifically, the lateral confinement is consistent with maintaining a suspended-sediment profile with elevated sediment concentrations nearer the bed and larger particle sizes nearer the bed. Both of these properties could lead the

observed sedimentation pattern in the westernmost channel for depositional turbidity currents. We propose that this pattern is not seen in Canyons 1, 2, and 3 because of up-dip adjustments to the characteristic suspended-sediment profile that occurs as the sediment gravity currents move across the unconfined segment of continental slope.

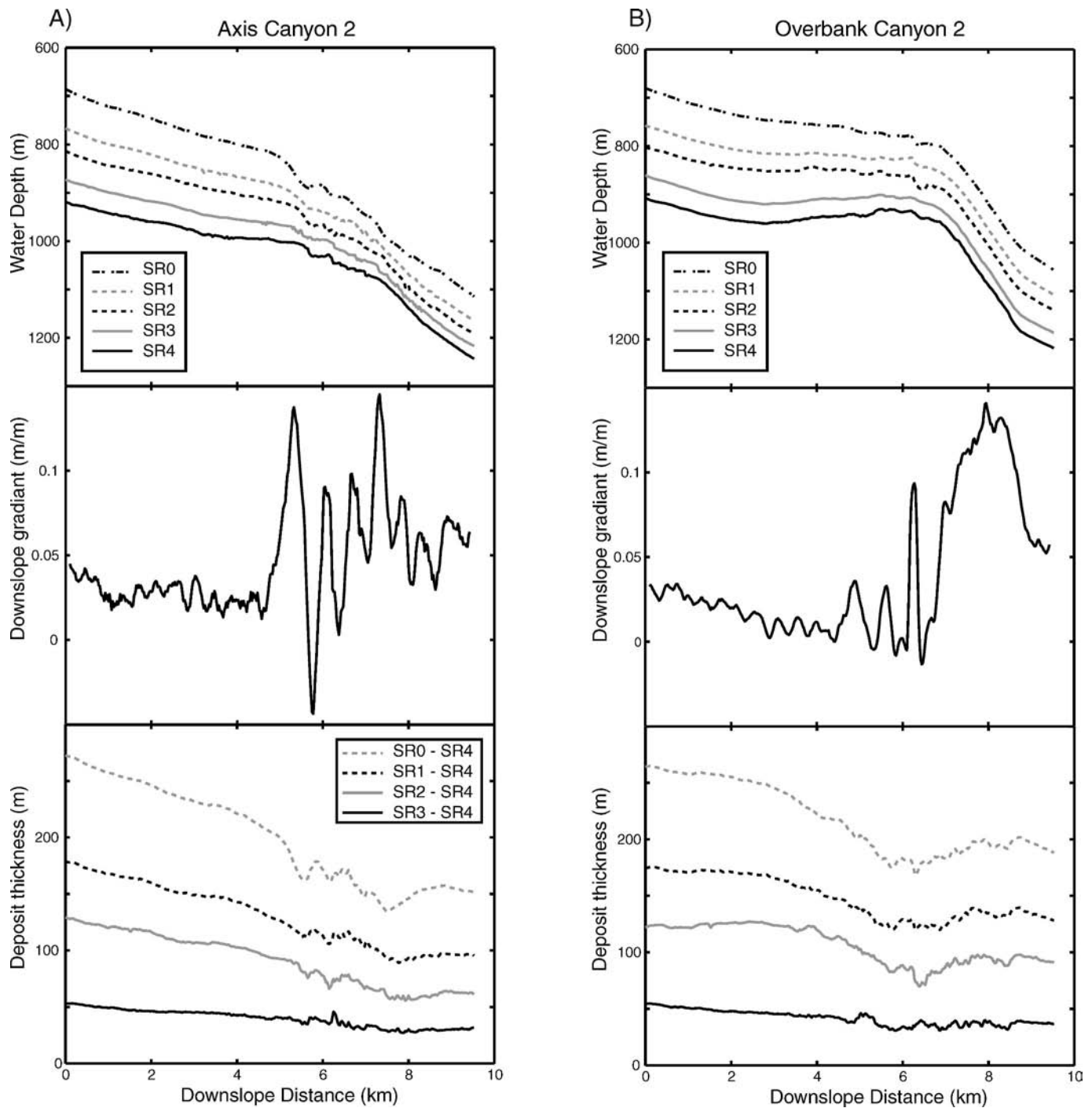


FIG. 11.—Comparison of properties for Canyon 2 and adjacent overbank at the shale ridge. **A-1)** Long profiles for seismic horizons SR4–SR0 following swath C2 (Fig. 3A) and the present-day axis of Canyon 2 (Fig. 1C). **A-2)** Surface gradient for the long profile of horizon SR0, the present-day seafloor, following the axis of Canyon 2. **A-3)** Deposit thickness measured between horizons SR4–SR1 along swath C2, the axis of Canyon 2. **B-1)** Representative long profiles for the overbank surface laterally adjacent to Canyon 2. Each profile represents the average elevation for seismic horizons SR4–SR0 along transects O2 and O3 (Fig. 3A). **B-2)** Downslope gradient of present-day seafloor associated with the average overbank profile in part B-1. **B-3)** Deposit thickness associated with successive long profiles in part B-1. The shaded region defines local minima in overbank sedimentation. See text for details.

Deepening of submarine canyons under net depositional conditions should asymptotically approach a steady-state canyon depth. Canyon deepening continues until its cross-sectional area is sufficient to collect all of the current, starving the intercanyon surface of current and its sediment supply. The maximum canyon depth in net depositional

environments would therefore depend on the flow and sediment-transporting properties of the sheet flows, including unconfined thickness, discharge, and sizes of suspended particles. A schematic illustration of the proposed model for development of constructional submarine canyons is presented in Figure 15.

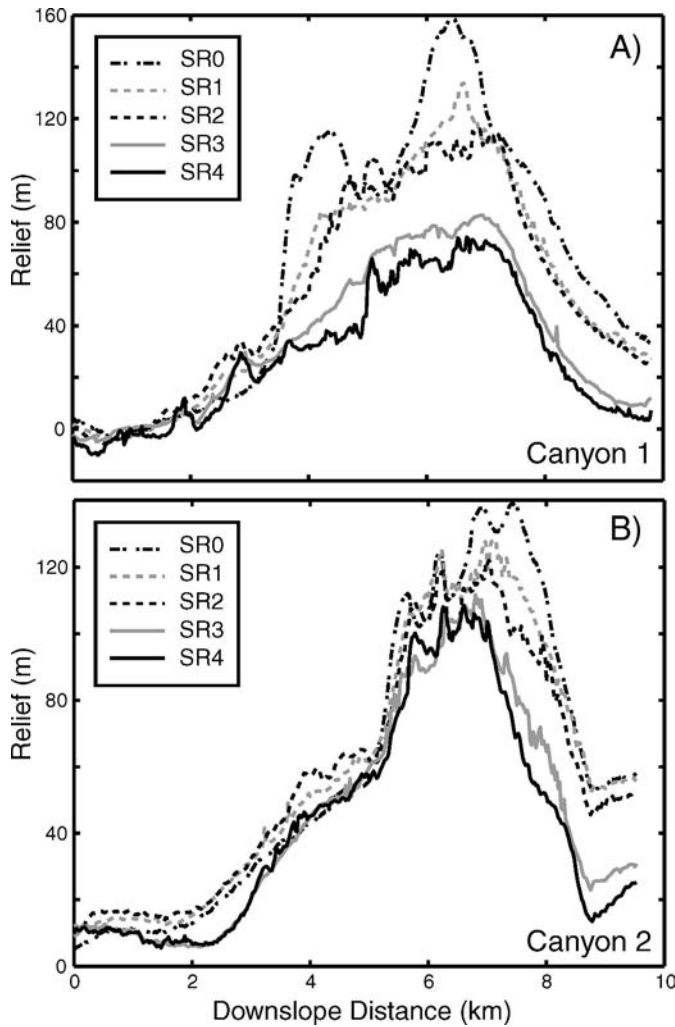


FIG. 12.— Plots defining down-canyon change in relief as a function of progressive sedimentation. Relief is defined as the difference in elevation of the average overbank surface and the canyon axis for seismic horizons SR4–SR0. **A)** Relief of Canyon 1 as a function of progressive sediment accumulation. Canyon axis and overbank surfaces defining relief are presented in Figs. 10A-1 and 10B-1. **B)** Relief of Canyon 2 with increasing sedimentation. Canyon axis and overbank surfaces defining relief are presented in Figures 11A-1 and 11B-1.

If deposition in our study region resulted from passage of sheet-like turbidity currents, our observations suggest that currents can adjust from dominantly channelized flows to dominantly sheet-like flows over relatively short length scales. Approximately 10 km upslope of our study region another shelf-edge-parallel shale ridge is observed and is also dissected by canyons. Assuming that flows are dominantly channelized when moving over this feature, flows would pass from channelized to sheet-like in less than 10 km.

**Turbidity-Current Thickness**

The cross-sectional area of the canyons traversing the shale-cored anticline (Fig. 4B) can be used to estimate a minimum thickness of sheet-like turbidity currents approaching the obstruction. Since deposition occurs on the bathymetric highs between canyons, the currents must be at least as thick as the maximum canyon relief while traversing the shale ridge. From Figure 4B we estimate the minimum cross-sectional area necessary the fill up the canyons and inundate highest intercanyon surface to be  $4 \times 10^5 \text{ m}^2$ . Evenly distributing this area across the unchannelized

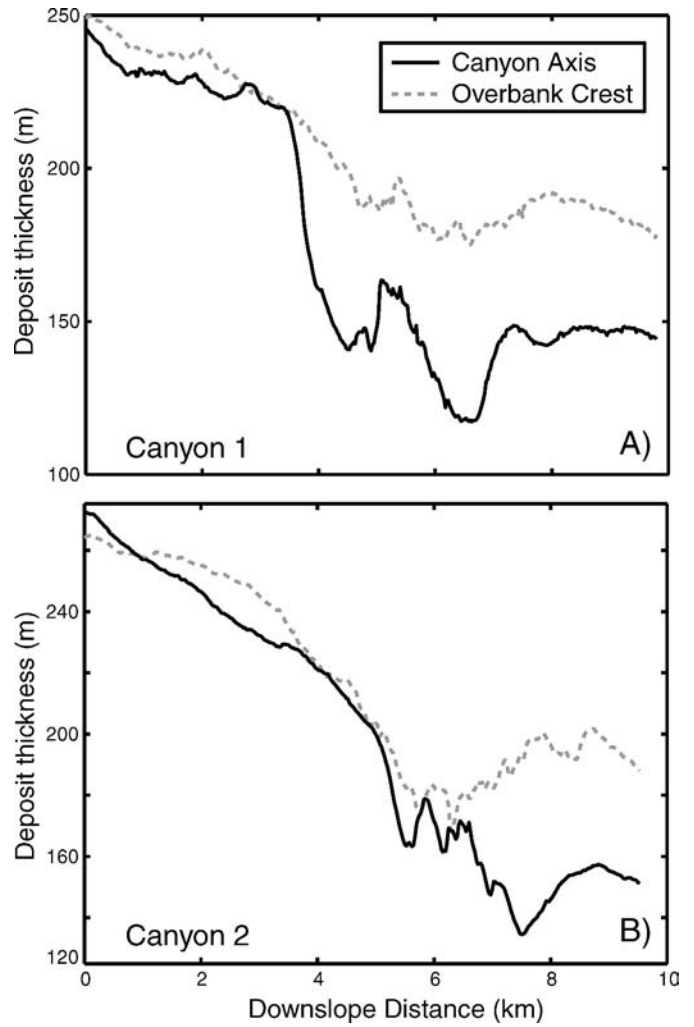


FIG. 13.— Comparison of deposit thickness for canyon axis and average overbank. Deposit thickness is measured between horizons SR4 and SR0. **A)** Canyon 1 profiles (see Fig. 10 for details). **B)** Canyon 2 profiles (see Fig. 11 for details).

slope updip from the shale ridge yields a minimum thickness of 20 m for the laterally extensive, sheet-like current.

**DISCUSSION**

This study illustrates that topographic morphologies traditionally attributed to net erosional environments can in fact develop under net depositional conditions in submarine settings. This observation has received recent attention because of the identification and characterization of submarine cyclic steps (Fildani et al. 2006; Sun and Parker 2005). Cyclic steps are bedform-like features with upstream and downstream bounding hydraulic jumps (Sun and Parker 2005). These features were assumed to be net erosional in character until recent studies by Winterwerp et al. (1992) and Taki and Parker (2005) observed their formation in net-depositional settings. Depositional cyclic steps have recently been identified offshore Monterey Bay, California, associated with flow stripped from partially channelized turbidity currents rounding a submarine channel bend (Fildani et al. 2006).

We propose that the depositional, step-like topography identified in the axes of canyons 1 and 2 are also cyclic steps (Figs. 10A-1, 11A-1). Seismic profiles along the axis of canyon 1 reveal large-scale bed roughness that is

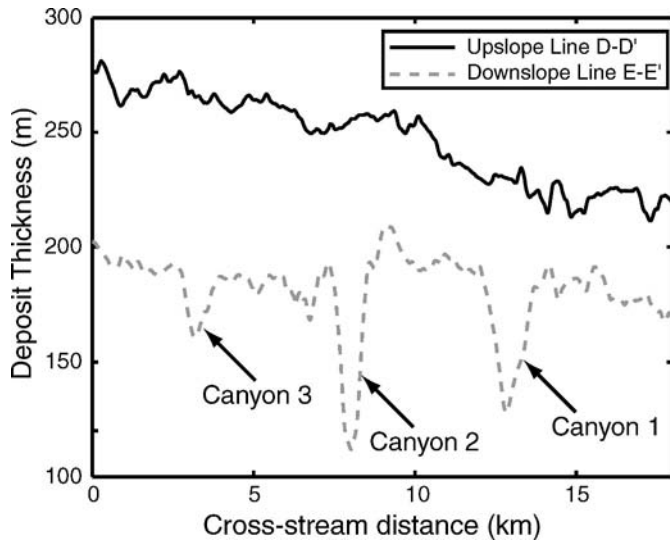


FIG. 14.—Strike profiles of deposit thickness measured upslope of shale ridge (line D–D' in Fig. 8C) and at the crest of the shale ridge (line E–E' in Fig. 8C). Deposit thickness is measured between horizons SR4 and SR0.

moving up slope through time, a characteristic of cyclic steps in depositional environments (Fig. 5). Identification of net-depositional features with seafloor characteristics frequently attributed to net-erosional processes has been made possible through the mapping of

subsurface stratigraphy in the 3-D seismic volume. This presents a potential problem for scientists studying regions where bathymetric maps are the only geological data available: how to infer dynamic processes from topographic data? Several recent studies have used purely erosional models of surface evolution to characterize seafloor topographic features where no subsurface data exist (Mitchell 2005, 2006). Our work illustrates that simply identifying the sign ( $\pm$ ) of evolution of surface topography is potentially fraught with errors and highlights the need for additional study into submarine transport processes.

Canyons traversing a shale ridge in our study region grew in relief during the Quaternary as a result of higher deposition rates on intercanyon topographic highs relative to canyon axes. Seismic horizons that extend in the strike direction for  $> 18$  km and deposits that thin with distance from the shelf edge suggest that canyon-forming currents were laterally extensive sheet flows. Laterally persistent stratigraphy likely deposited by sheet-flows highlights critical differences in transport properties of terrestrial rivers and submarine turbidity currents. In the terrestrial environment, the high density of the transporting fluid (water) relative to the ambient fluid (air) results in flows that are more strongly affected by and confined to local topography when compared against turbidity currents. As a result, terrestrial overbank environments, in regions of relative uplift and canyon formation, are seldom inundated by sediment-depositing flows, and increases in relief require focused erosion within canyons. In contrast, the low excess density of turbidity currents allows a significant quantity of a significantly large flow to traverse over intercanyon highs without being funneled into canyons, thereby supplying overbank regions with sediment to counter deposition occurring within canyons (Fig. 16).

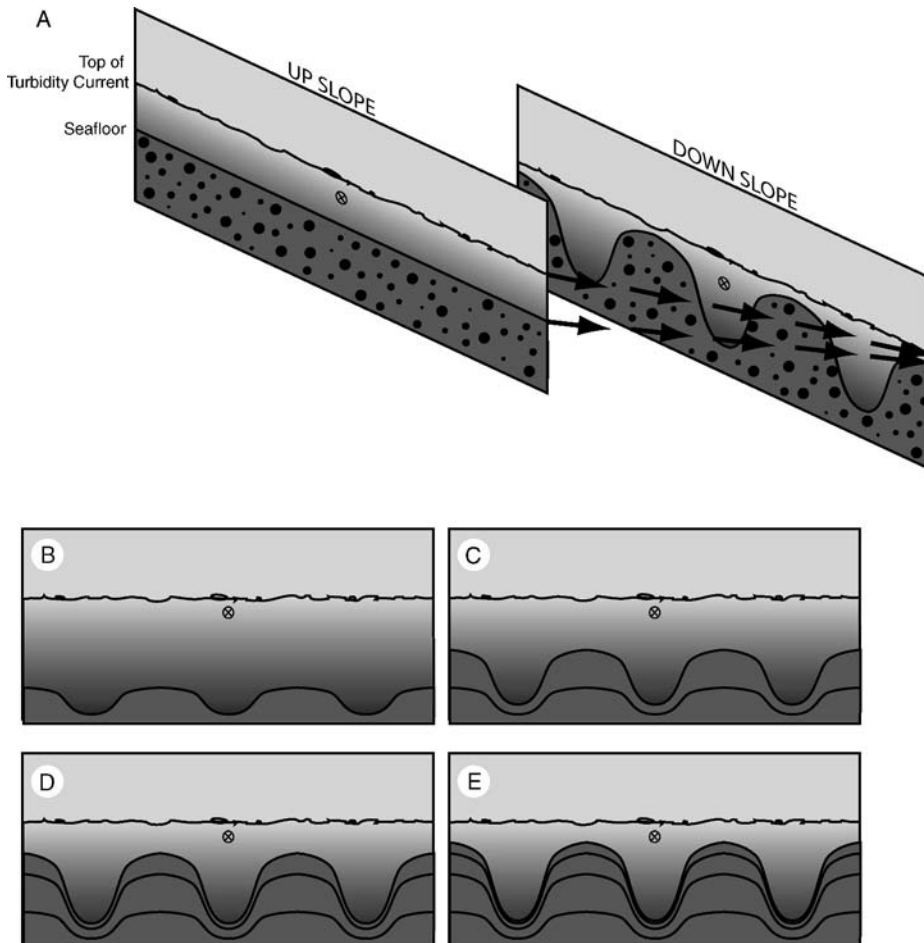


FIG. 15.—Conceptual illustrations of how sheet-like turbidity currents could interact with the growing shale ridge to produce constructional canyons. A) Sheet-like current upslope of shale ridge and filling canyons at the crest-line of the shale ridge. The cross-sectional area of the current is the same at both positions. B–E) Proposed evolution of shale-ridge and canyon topography associated with net-depositional, sheet-like turbidity currents. Canyon relief increases through time because sedimentation is always greatest on the unconfined surfaces separating the canyons from each other. As canyon relief increases, deposition decreases on these overbank surfaces. Sediment accumulation at the canyon axes also decreases with increasing canyon relief.

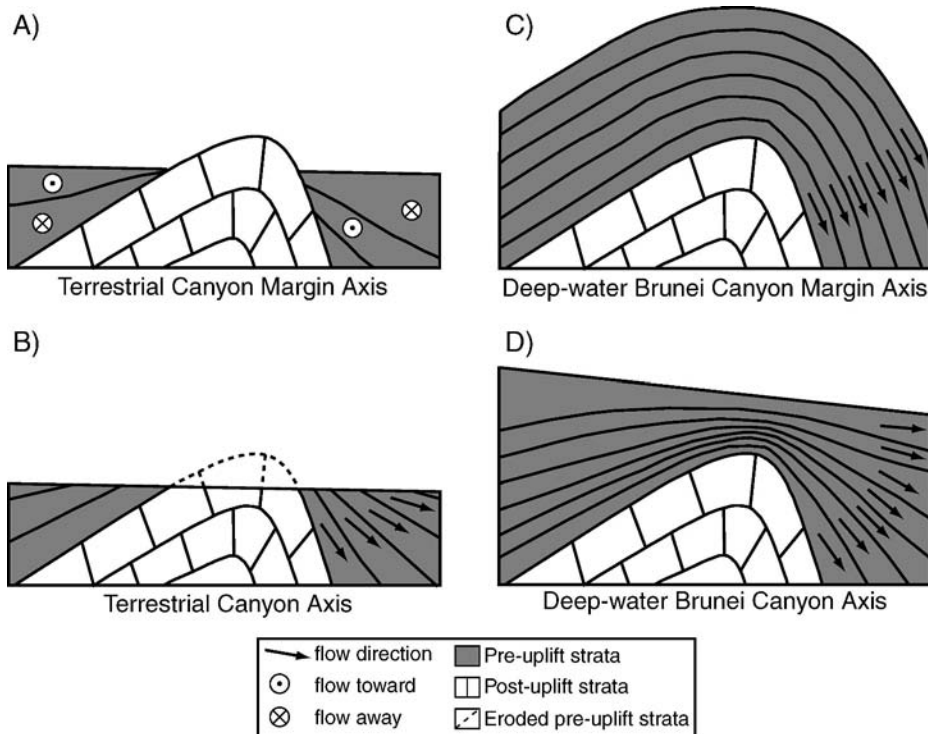


FIG. 16.—Stratigraphic characteristics related to rivers and submarine channels that are antecedent to a growing structure. **A)** Schematic stratigraphic cross section following the over-bank profile of a terrestrial canyon. Deposition by migrating channels keeps pace with erosion upslope and downslope of the anticline hinge, but the uplift rate surpasses the deposition rate at the anticline hinge. **B)** Cross section following a terrestrial canyon axis. The channel is depositional upslope and downslope of the anticline hinge but erosional over the hinge axis. **C)** Cross section following the overbank profile of a submarine canyon. Uplift of the anticline does not significantly alter downslope deposition trends. **D)** Cross section following a submarine-canyon axis. Uplift of the anticline forces local minima in downslope deposition trends centered over the position of maximum uplift.

The mechanism(s) responsible for initiating currents in excess of 20 m thick and 18 km wide is unknown for this region. Today a continental shelf 50–70 km wide separates the major regional rivers from the continental shelf edge, suggesting that a direct feed of sediment from rivers to the deep marine by hyperpycnal events is unlikely at times of relatively high sea level (Mulder et al. 2003). In addition, seismic cross sections through the present-day continental shelf directly updip from the study area do not preserve a record of a direct fluvial link to the shelf edge during Quaternary sea-level lowstands. This suggests that the sediment composing the large turbidity currents has a nontrivial residence time on the continental shelf prior to movement down the slope. Studies from the continental shelves offshore the Amazon River (Trowbridge and Kineke 1994; Kineke et al. 1996) and the Eel River (Traykovski et al. 2000) demonstrated the ability of fine-grained sediment to be re-entrained as fluid muds by normal wave and current activity. Flow of fluid muds over the Borneo continental shelf edge triggered by large storms or some other unknown mechanism is likely to be the source of sediment for the canyon constructing sheet flows in our study region.

#### SUMMARY

Submarine canyons are often assumed to be sites of net erosion (Huyghe et al. 2004; Cunningham et al. 2005). This assumption is derived from surface evolution models constructed from observations of terrestrial canyons (Burbank et al. 1996; Burbank and Pinter 1999; Humphrey and Konrad 2000). In this study, mapping of subsurface stratigraphy over a shale-cored anticline has revealed submarine canyons that deepened under conditions of net sediment deposition.

Submarine fans offshore large river systems such as the northern Borneo continental margin record the highest long-term deposition rates of any submarine feature (Bouma et al. 1985). Continental slopes incorporated in these fans possess many topographic elements that are morphologically similar to terrestrial erosional features (Pirmez 1994; Greene et al. 2002). This work demonstrates that submarine canyons, which might be interpreted as erosional features after analysis of only the present-day seafloor, can in some cases be net-depositional features. The

difficulties inherent in directly measuring the processes responsible for crafting continental-slope morphologies increase the need for remotely sensed images of the subsurface. These seismic volumes allow the scientific community studying submarine environments to ground-truth interpretations of processes which craft these margins.

#### ACKNOWLEDGMENTS

We thank Brunei Shell Petroleum and Abd-Razak Damit for permission to publish seismic data from offshore Brunei Darussalam. Support for our research was provided by the STC Program of the National Science Foundation via the National Center for Earth-Surface Dynamics under Agreement Number EAR-0120914. Carlos Pirmez and the Shell Turbidite Research Group provided valuable help and stimulating discussions in the early stages of the project. Finally, we thank Bill McCaffrey, Russell Wynn, and Dave McGee for constructive reviews which greatly improved this manuscript.

#### REFERENCES

- BERTONI, C., AND CARTWRIGHT, J., 2005, 3D seismic analysis of slope-confined canyons from the Plio-Pleistocene of the Ebro Continental Margin (Western Mediterranean): *Basin Research*, v. 17, p. 43–62.
- BEST, J.L., KOSTASCHUK, R.A., PEAKALL, J., VILLARD, P.V., AND FRANKLIN, M., 2005, Whole flow field dynamics and velocity pulsing within natural sediment-laden underflows: *Geology*, v. 33, p. 765–768.
- BOOTH, J.R., DUVERNAY, A.E., PREIFFER, D.S., AND STYZEN, M.J., 2000, Sequence stratigraphic framework, depositional models, and stacking patterns of ponded and slope fan systems in the Auger Basin: Central Gulf of Mexico Slope: SEPM, Gulf Coast Section, 20th Annual Research Conference, Deep-Water Reservoirs of the World, p. 82–103.
- BOUMA, A., NORMARK, W.R., AND BARNES, N.E., 1985, *Submarine Fans and Related Turbidite Systems*: New York, Springer Verlag, 351 p.
- BURBANK, D.W., AND PINTER, N., 1999, Landscape evolution: the interactions of tectonics and surface processes: *Basin Research*, v. 11, p. 1–6.
- BURBANK, D.W., MEIGS, A., AND BROZOVIC, N., 1996, Interactions of growing folds and coeval depositional systems: *Basin Research*, v. 8, p. 199–223.
- BURBANK, D.W., McLEAN, J.K., BULLEN, M., ABDRAKHMATOV, K.Y., AND MILLER, M.M., 1999, Partitioning of intermontane basins by thrust-related folding, Tien Shan, Kyrgyzstan: *Basin Research*, v. 11, p. 75–92.

- CACCHIONE, D.A., PRATSON, L., AND OGSTON, A.S., 2002, The shaping of continental slopes by internal tides: *Science*, v. 296, p. 724–727.
- CANALS, M., CASAMOR, J.L., URGELES, R., LASTRAS, G., CALAFAT, A.M., MASSON, D.G., BERNE, S., AND ALONSO, B., 2000, The Ebro Continental Margin, Western Mediterranean Sea: Interplay Between Canyon-Channel Systems and Mass Wasting Processes: SEPM, Gulf Coast Section, 20th Annual Research Conference, Deep-Water Reservoirs of the World, p. 152–174.
- CUNNINGHAM, M.J., HODGSON, S., MASSON, D.G., AND PARSON, L.M., 2005, An evaluation of along- and down-slope sediment transport processes between Goban Spur and Brenot Spur on the Celtic Margin of the Bay of Biscay: *Sedimentary Geology*, v. 179, p. 99–116.
- DEMYTTENAERE, R., TROMP, J.P., IBRAHIM, A., ALLMAN-WARD, P., AND MECKEL, T., 2000, Brunei deep water exploration: from sea floor images and shallow seismic analogues to depositional models in a slope-turbidite setting: SEPM, Gulf Coast Section, 20th Annual Research Conference, Deep-Water Reservoirs of the World, p. 304–317.
- FIELD, M.E., GARDNER, J.V., AND PRIOR, D.B., 1999, Geometry and significance of stacked gullies on the northern California slope: *Marine Geology*, v. 154, p. 271–286.
- FILDANI, A., AND NORMARK, W.R., 2004, Late Quaternary evolution of channel and lobe complexes of Monterey Fan: *Marine Geology*, v. 206, p. 199–223.
- FILDANI, A., NORMARK, W.R., KOSTIC, S., AND PARKER, G., 2006, Channel formation by flow stripping: large-scale scour features along the Monterey East Channel and their relation to sediment waves: *Sedimentology*, v. 53, p. 1–23.
- FORNENTO-TRIGILIO, M.L., BURBANK, D.W., NICOL, A., SHULMEISTER, J., AND RIESER, U., 2002, River response to an active fold-and-thrust belt in a convergent margin setting, North Island, New Zealand: *Geomorphology*, v. 49, p. 125–152.
- GARCIA, M., ALONSO, B., ERCILLA, G., AND GRACIA, E., 2005, The tributary valley systems of the Almería Canyon (Alboran Sea, SW Mediterranean): sedimentary architecture: *Marine Geology*, v. 226, p. 207–223.
- GOFF, J.A., 2001, Quantitative classification of canyon systems on continental slopes and a possible relationship to slope curvature: *Geophysical Research Letters*, v. 28, p. 4359–4362.
- GREENE, H.G., MAHER, N.M., AND PAULL, C.K., 2002, Physiography of the Monterey Bay National Marine Sanctuary and implications about continental margin development: *Marine Geology*, v. 181, p. 55–82.
- HAY, A.E., 1987, Turbidity currents and submarine channel formation in Rupert Inlet, British Columbia. 2. The role of continuous and surge-type flow: *Journal of Geophysical Research*, v. 92, p. 2883–2900.
- HISCOTT, R.N., 2001, Depositional sequences controlled by high rates of sediment supply, sea-level variations, and growth faulting: the Quaternary Baram Delta of northwestern Borneo: *Marine Geology*, v. 175, p. 67–102.
- HUMPHREY, N.F., AND KONRAD, S.K., 2000, River incision or diversion in response to bedrock uplift: *Geology*, v. 28, p. 43–46.
- HUTCHISON, C.S., 2004, Marginal basin evolution: the southern South China Sea: *Marine and Petroleum Geology*, v. 21, p. 1129–1148.
- HUYGHE, P., FOATA, M., DEVILLE, E., MASCLE, G., AND GROUP, C.W., 2004, Channel profiles through the active thrust front of the southern Barbados prism: *Geology*, v. 32, p. 429–432.
- IMRAN, J., PARKER, G., AND PIRMEZ, C., 1999, A non-linear model of flow in meandering submarine and subaerial channels: *Journal of Fluid Mechanics*, v. 400, p. 295–331.
- IMRAN, J., KASSEM, A., AND KHAN, S.M., 2004, Three-dimensional modeling of density current. I. Flow in straight confined and unconfined channels: *Journal of Hydraulic Engineering*, v. 42, p. 578–590.
- INGRAM, G.M., CHISHOLM, T.J., GRANT, C.J., HEDLUND, C.A., STUART-SMITH, P., AND TEASDALE, J., 2004, Deepwater North West Borneo: hydrocarbon accumulation in an active fold and thrust belt: *Marine and Petroleum Geology*, v. 21, p. 879–887.
- KEEVIL, G.M., PEAKALL, J., BEST, J.L., AND AMOS, K.J., 2006, Flow structure in sinuous submarine channels: Velocity and turbulence structure of an experimental submarine channel: *Marine Geology*, v. 229, p. 241–257.
- KHRIPOUNOFF, A., VANGRIESHEIM, A., BABONNEAU, N., CRASSOUS, P., DENNIELOU, B., AND SAVOYE, B., 2003, Direct observations of intense turbidity current activity in the Zaire submarine valley at 4000 m water depth: *Marine Geology*, v. 194, p. 151–158.
- KINEKE, G.C., STERNBERG, R.W., TROWBRIDGE, J.H., AND GEYER, W.R., 1996, Fluid-mud processes on the Amazon continental shelf: *Continental Shelf Research*, v. 16, p. 667–696.
- KNELLER, B., AND BUCKEE, C.M., 2000, The structure and fluid mechanics of turbidity currents: a review of some recent studies and their geological implications: *Sedimentology*, v. 47, p. 62–94.
- KNELLER, B., EDWARDS, D., McCAFFREY, W., AND MOORE, R., 1991, Oblique reflection of turbidity currents: *Geology*, v. 19, p. 250–252.
- KOMAR, P.D., 1969, The channelized flow of turbidity currents with application to Monterey Deep-Sea Channel: *Journal of Geophysical Research*, v. 71, p. 4544–4558.
- LAMB, M.P., TONIOLO, H., AND PARKER, G., 2006, Trapping of sustained turbidity currents by intraslope minibasins: *Sedimentology*, v. 53, p. 147–160.
- LAMB, M.P., PARSONS, J.D., MULLENBACH, B.L., FINLAYSON, D.P., ORANGE, D.L., AND NITTROUER, C.A., 2008, Evidence for superelevation, channel incision, and formation of cyclic steps by turbidity currents in Eel Canyon, California: *Geological Society of America, Bulletin*, v. 120, p. 463–475.
- LAWS, E.A., FALKOWSKI, P.G., SMITH, W.O., DUCKLOW, H., AND MCCARTHY, J.J., 2000, Temperature effects on export production in the open ocean: *Global Biogeochemical Cycles*, v. 14, p. 1231–1246.
- MCGILVER, T.A., AND COOK, D.L., 2003, The influence of local gradients on accommodation space and linked depositional elements across a stepped slope profile, offshore Brunei, in Roberts, H., ed., *Shelf Margin Deltas and Linked Down Slope Petroleum Systems: Global Significance and Future Exploration Potential*, SEPM, Gulf Coast Section, 23rd Annual Bob F. Perkins Research Conference, p. 387–419.
- MITCHELL, N.C., 2005, Interpreting long-profiles of canyons in the USA Atlantic continental slope: *Marine Geology*, v. 214, p. 75–99.
- MITCHELL, N.C., 2006, Morphologies of knickpoints in submarine canyons: *Geological Society of America, Bulletin*, v. 118, p. 589–605.
- MOHRIG, D., AND BUTTLES, J., 2007, Shallow channels constructed by deep turbidity currents: *Geology*, v. 35, p. 155–158.
- MORLEY, C.K., 2007, Interaction between critical wedge geometry and sediment supply in a deep-water fold belt: *Geology*, v. 35, p. 139–142.
- MULDER, T., SYVITSKI, J.P.M., MIGEON, S., FAUGERES, J., AND SAVOYE, B., 2003, Marine hyperpycnal flows: initiation, behavior and related deposits. A review: *Marine and Petroleum Geology*, v. 20, p. 861–882.
- PEAKALL, J., McCAFFREY, B., AND KNELLER, B., 2000, A process model for the evolution, morphology, and architecture of sinuous submarine channels: *Journal of Sedimentary Research*, v. 70, p. 434–448.
- PICKERING, K.T., UNDERWOOD, M.B., AND TAIRA, A., 1992, Open-ocean to trench turbidity-current flow in the Nankai Trough: flow collapse and reflection: *Geology*, v. 20, p. 1099–1102.
- PIPER, D.J.W., AND NORMARK, W.R., 1983, Turbidite depositional patterns and flow characteristics, Navy submarine fan, California Borderland: *Sedimentology*, v. 30, p. 681–694.
- PIRMEZ, C., 1994, Growth of a submarine meandering channel-levee system on the Amazon Fan [Ph.D. thesis]: Columbia University, 621 p.
- PIRMEZ, C., AND FLOOD, R.D., 1995, Morphology and structure of Amazon channel, in Flood, R.D., Piper, D.J.W., Klaus, A., and Peterson, L.C., eds., *Proceedings of the Ocean Drilling Program, Initial Results: College Station, Texas, Ocean Drilling Program*, p. 23–45.
- PIRMEZ, C., AND IMRAN, J., 2003, Reconstruction of turbidity currents in Amazon Channel: *Marine and Petroleum Geology*, v. 20, p. 823–849.
- PIRMEZ, C., BEAUBOUF, R.T., FRIEDMANN, S.J., AND MOHRIG, D., 2000, Equilibrium profile and baselevel in submarine channels: examples from late Pleistocene systems and implications for the architecture of deepwater reservoirs: SEPM, Gulf Coast Section, 20th Annual Research Conference, Deep-Water Reservoirs of the World, p. 782–805.
- POSAMANTIER, H.W., AND KOLLA, V.E., 2003, Seismic geomorphology and stratigraphy of depositional elements in deep-water settings: *Journal of Sedimentary Research*, v. 73, p. 367–388.
- PRATSON, L., AND HAXBY, W.F., 1996, What is the slope of the U.S. continental slope?: *Geology*, v. 24, p. 3–6.
- PRATSON, L., RYAN, W.B.F., MOUNTAIN, G.S., AND TWITCHELL, D.C., 1994, Submarine canyon initiation by downslope-eroding sediment flows: evidence in late Cenozoic strata on the New Jersey continental slope: *Geological Society of America, Bulletin*, v. 106, p. 395–412.
- RIBBE, J., AND HOLLOWAY, P.E., 2001, A model of suspended sediment transport by internal tides: *Continental Shelf Research*, v. 21, p. 395–422.
- SALLER, A., AND BLAKE, G., 2003, Sequence stratigraphy and syndepositional tectonics of upper Miocene and Pliocene deltaic sediments, offshore Brunei Darussalam, in Hasan Sidi, F., ed., *Tropical Deltas of Southeast Asia—Sedimentology, Stratigraphy, and Petroleum Geology*, SEPM, Special Publication 76, p. 219–234.
- SANDAL, S.T., 1996, The geology and hydrocarbon resources of Negara Brunei Darussalam: Brunei Darussalam, Brunei Shell Petroleum Company Sendirian Berhad and Brunei Museum, 243 p.
- SKENE, K.I., PIPER, D.J.W., AND HILL, P.S., 2002, Quantitative analysis of variations in depositional sequence thickness from submarine channel levees: *Sedimentology*, v. 49, p. 1411–1430.
- SMITH, D.P., RUIZ, G., KVITEK, R., AND IAMPIETRO, P.J., 2005, Semiannual patterns of erosion and deposition in upper Monterey Canyon from serial multibeam bathymetry: *Geological Society of America, Bulletin*, v. 117, p. 1123–1133.
- SNYDER, N.P., WHIPPLE, K.X., TUCKER, G.E., AND MERRITTS, D.J., 2000, Landscape response to tectonic forcing: digital elevation model analysis of stream profiles in the Mendocino triple junction region, northern California: *Geological Society of America, Bulletin*, v. 112, p. 1250–1263.
- SPINNELLI, G.A., AND FIELD, M.E., 2001, Evolution of continental slope gullies on the northern California margin: *Journal of Sedimentary Research*, v. 71, p. 237–245.
- STELTING, C.W., PICKERING, K., BOUMA, A., COLEMAN, J.M., CREMER, M., DROZ, L., MEYER-WRIGHT, A.A., NORMARK, W.R., O'CONNELL, S., STOW, D.A., AND SCIENTISTS, D.L.S., 1985, Drilling results on the Middle Mississippi Fan, in Bouma, A., Barnes, N.E., and Normark, W.R., eds., *Submarine Fans and Related Turbidite Sequences: New York, Springer-Verlag*, p. 275–282.
- STOW, D.A.V., HUC, A.-Y., AND BERTRAND, P., 2001, Depositional processes of black shales in deep water: *Marine and Petroleum Geology*, v. 18, p. 491–498.
- STRAUB, K.M., AND MOHRIG, D., in press, Quantifying the morphology and growth of levees in aggrading submarine channels: *Journal of Geophysical Research, Earth Surface*.
- STRAUB, K.M., JEROLMACK, D.J., MOHRIG, D., AND ROTHMAN, D.H., 2007, Channel network scaling laws in submarine basins: *Geophysical Research Letters*, v. 34, ISI:000247682100003.

- STRAUB, K.M., MOHRIG, D., MCELROY, B., BUTTLES, J., AND PIRMEZ, C., 2008, Interactions between turbidity currents and topography in aggrading sinuous submarine channels: A laboratory study: *Geological Society of America, Bulletin*, v. 120, p. 368–385.
- SUN, T., AND PARKER, G., 2005, Transportational cyclic steps created by flow over an erodible bed. Part 2. Theory and numerical simulation: *Journal of Hydraulic Research*, v. 43, p. 502–514.
- TAKI, K., AND PARKER, G., 2005, Transportational cyclic steps created by flow over an erodible bed. Part 1. Experiments: *Journal of Hydraulic Research*, v. 43, p. 488–501.
- TRAYKOVSKI, P., GEYER, W.R., IRISH, J.D., AND LYNCH, J.F., 2000, The role of wave-induced density-driven fluid mud flows for cross-shelf transport on the Eel River continental shelf: *Continental Shelf Research*, v. 20, p. 2113–2140.
- TROWBRIDGE, J.H., AND KINEKE, G.C., 1994, Structure and dynamics of fluid muds on the Amazon continental shelf: *Journal of Geophysical Research*, v. 99, p. 865–874.
- TUCKER, G.E., AND SLINGERLAND, R.L., 1996, Predicting sediment flux from fold and thrust belts: *Basin Research*, v. 8, p. 329–350.
- TWITCHELL, D.C., CROSS, V.A., HANSON, A.D., BUCK, B.J., ZYBALA, J.G., AND RUDIN, M.J., 2005, Seismic architecture and lithofacies of turbidites in Lake Mead (Arizona and Nevada, U.S.A.), an analogue for topographically complex basins: *Journal of Sedimentary Research*, v. 75, p. 134–148.
- VAN RENSBURGEN, P., MORLEY, C.K., ANG, D.W., HOAN, T.Q., AND LAM, N.T., 1999, Structural evolution of shale diapirs from reactive rise to mud volcanism: 3D seismic data from the Baram delta, offshore Brunei, Darussalam: *Journal of the Geological Society of London*, v. 156, p. 633–650.
- VIOLET, J., SHEETS, B., PRATSON, L., PAOLA, C., BEAUBOUF, R.T., AND PARKER, G., 2005, Experiment on turbidity currents and their deposits in a model 3D subsiding minibasin: *Journal of Sedimentary Research*, v. 75, p. 820–843.
- WESTBROOK, G.K., AND SMITH, M.J., 1983, Long décollements and mud volcanoes: Evidence from the Barbados Ridge Complex for the role of high pore-fluid pressure in the development of an accretionary complex: *Geology*, v. 11, p. 279–283.
- WINTERWERP, J.C., BAKKER, W.T., MASTBERGEN, D.R., AND VAN ROSSUM, H., 1992, Hyperconcentrated sand-water mixture flows over erodible bed: *Journal of Hydraulic Engineering*, v. 119, p. 1508–1525.
- WRIGHT, L.D., WISEMAN, W.J.J., BORNHOLD, B.D., PRIOR, D.B., SUHAYDA, J.N., KELLER, G.H., YANG, L.S., AND FAN, Y.B., 1988, Marine dispersal and deposition of Yellow River silts by gravity-driven underflows: *Nature*, p. 629–632.
- WYNN, R.B., MASSON, D.G., STOW, D.A.V., AND WEAVER, P.P.E., 2000a, Turbidity current sediment waves on the submarine slopes of the western Canary Islands: *Marine Geology*, v. 163, p. 185–198.
- WYNN, R.B., WEAVER, P.P.E., ERCILLA, G., STOW, D.A.V., AND MASSON, D.G., 2000b, Sedimentary processes in the Selvage sediment-wave field, NE Atlantic: new insights into the formation of sediment waves by turbidity currents: *Sedimentology*, v. 47, p. 1181–1197.
- XU, J.P., NOBLE, M.A., AND ROSENFELD, L.K., 2004, In-situ measurements of velocity structure within turbidity currents: *Geophysical Research Letters*, v. 31, ISI:000221473000005.

Received 18 August 2007; accepted 15 July 2008.